Appl Microbiol Biotechnol (2014) 98:9499–9515
DOI 10.1007/s00253-014-6093-9

BIOENERGY AND BIOFUELS

Biochemical, genetic, and metabolic engineering strategies to enhance coproduction of 1-propanol and ethanol in engineered *Escherichia coli*

Kajan Srirangan · Xuejia Liu · Adam Westbrook · Lamees Akawi · Michael E. Pyne · Murray Moo-Young · C. Perry Chou

Received: 21 July 2014 / Revised: 8 September 2014 / Accepted: 10 September 2014 / Published online: 10 October 2014

Abstract We recently reported the heterologous production of 1-propanol in *Escherichia coli* via extended dissimilation of succinate under anaerobic conditions through expression of the endogenous sleeping beauty mutase (Sbm) operon. In the present work, we demonstrate high-level coproduction of 1-propanol and ethanol by developing novel engineered *E. coli* strains with effective cultivation strategies. Various biochemical, genetic, metabolic, and physiological factors affecting relative levels of acidogenesis and solventogenesis during anaerobic fermentation were investigated. In particular, CPC-PrOH3, a plasmid-free propanogenic *E. coli* strain derived by activating the Sbm operon on the genome, showed high levels of solventogenesis accounting for up to 85 % of dissimilated carbon. Anaerobic fed-batch cultivation of CPC-PrOH3 with glycerol as the major carbon source produced high titers of nearly 7 g/L 1-propanol and 31 g/L ethanol, implying its potential industrial applicability. The activated Sbm pathway served as an ancillary channel for consuming reducing equivalents upon anaerobic dissimilation of glycerol, resulting in an enhanced glycerol dissimilation and a major metabolic shift from acidogenesis to solventogenesis.

Keywords Biofuel · *Escherichia coli* · Genomic engineering · Glycerol · Metabolic engineering · 1-Propanol

K. Srirangan · X. Liu · A. Westbrook · L. Akawi · M. E. Pyne · M. Moo-Young · C. P. Chou (✉)
Department of Chemical Engineering, University of Waterloo, 200 University Avenue West, Waterloo, Ontario, Canada N2L 3G1
e-mail: cpchou@uwaterloo.ca

Introduction

1-Propanol is a C3-primary alcohol with broad industrial applicability, serving as a precursor for the production of several commodity chemicals (e.g., diesel fuels and propylene) and a general solvent in the pharmaceutical and textile industries for the formulation of drugs, antiseptic solutions, cosmetics, and dyes (Fiege et al. 2002). In addition, several physical and chemical properties make 1-propanol superior to ethanol as an alternative biofuel (Fernando et al. 2007). 1-Propanol is produced primarily by petrochemical processes, such as Oxo synthesis, which is currently the most cost-effective approach (Rase 2000). Due to rising environmental concerns and finite crude oil reserves, a recent paradigm is the development of biotechnological (particularly, microbial) platforms for the production of biofuels, high-value commodities, and fine chemicals (Fernando et al. 2007; Jarboe et al. 2010; Rase 2000; Srirangan et al. 2012). Cultivation of engineered microorganisms with low-cost renewable feedstock for sustainable biofuel production may eventually displace existing fossil fuel technologies.

While no microorganisms have been identified as natural producers of 1-propanol, technological advances in synthetic biology and metabolic engineering have enabled the production of 1-propanol using engineered strains of *Escherichia coli*. For example, the L-threonine (Atsumi et al. 2008b; Jun Choi et al. 2012; Shen and Liao 2008) and citramalate (Atsumi et al. 2008a) pathways have been exploited for 1-propanol biosynthesis. Subsequently, synergistic coupling of the two pathways was shown to further enhance the production (Shen and Liao 2013). Furthermore, expansion of the canonical 1,2-propanediol pathway was explored by dehydrating and subsequently reducing 1,2-propanediol to 1-propanol (Jain and Yan 2011). Alternatively, Deng and Fong

(2011) reported the production of 1-propanol from a selection of lignocellulosic feedstocks using metabolically engineered *Thermobifida fusca*. Recently, we proposed a novel approach for 1-propanol production through extended dissimilation of the tricarboxylic acid (TCA) cycle intermediate of succinate (Srirangan et al. 2013) (Fig. 1). This was accomplished by converting succinate first to succinyl-CoA via succinyl-CoA synthase, subsequently to propionyl-CoA via enzymes associated with the sleeping beauty mutase (Sbm) operon (Haller et al. 2000), and finally to 1-propanol via bifunctional alcohol/aldehyde dehydrogenases. Specifically, the Sbm operon contains three key genes: (1) *sbm*, encoding a vitamin B_{12}-dependent methylmalonyl-CoA mutase for the isomerization of succinyl-CoA to L-methylmalonyl-CoA, (2) *ygfG*, encoding a methylmalonyl-CoA decarboxylase for decarboxylation of L-methylmalonyl-CoA to propionyl-CoA, and (3) *ygfH*, encoding a propionyl-CoA::succinate transferase facilitating the interconversion between succinyl-CoA and propionyl-CoA. The operon also contains a putative protein kinase (encoded by *ygfD*) whose molecular function remains largely unclear (Haller et al. 2000; Kannan 2008). The Sbm operon exists in the wild-type *E. coli* genome, but its expression remains minimal due to an inherently weak or inactive promoter (Froese et al. 2009; Haller et al. 2000), such that wild-type *E. coli* strains do not produce 1-propanol. Using our engineered *E. coli* strains, production titers up to 150 mg/L of 1-propanol were achieved in shake-flask cultures. However, the culture performance was limited due to a disproportionate channeling of central metabolic intermediates for the production of by-products such as lactate, acetate, and ethanol (Srirangan et al. 2013).

In the present study, we extended our exploration in strain engineering and cultivation strategies to identify various biochemical and genetic factors limiting 1-propanol production. The physiological and metabolic effects associated with host genotype and the expression of the Sbm operon under different culture conditions were investigated. In particular, based on an overall redox balance with respect to the fermentative metabolic network, the selection of a major carbon source for cultivation was identified to critically affect relative levels of acidogenesis and solventogenesis with a significant implication on 1-propanol production. On the other hand, while heterologous genes can be conveniently introduced into host cells via plasmids for cellular manipulation, the presence of multicopy plasmids often imposes a severe metabolic burden to cells and/or may result in various technical issues arising from structural and segregational plasmid instability, ultimately leading to retarded cell growth and diminished product formation. With recent technological advances in genomic engineering, plasmid-free systems can be more suitable for biomanufacturing purposes, particularly from the standpoint of metabolic engineering applications for which gene dosage is unlikely a limiting factor (Glick 1995; Jones et al. 2000; Ow et al. 2006). Herein, we also report the derivation of a plasmid-free propanogenic *E. coli* strain by activating the chromosomal Sbm operon for high-level coproduction of 1-propanol and ethanol.

Fig. 1 **a** Major metabolic pathways for anaerobic fermentation and the activated Sbm pathway for extended dissimilation of succinate to form 1-propanol. Enzymes catalyzing primary (*solid lines*) and divergent (*dashed lines*) reactions and the corresponding products are listed. (*I*) phosphotransferase system (PTS) enzyme I (*ptsI*), (*II*) histidine-containing protein (*ptsH*), (*III*) PTS enzyme $IIA^{glucose}$ (*crr*), (*1*) PTS enzyme $IIBC^{glucose}$ (*ptsG*): D-glucose-6-P, (*2*) glucosephosphate isomerase (*pgi*): D-fructose-6-P, (*3*) 6-phosphofructokinase I/II (*pfkAB*): fructose-1,6-BP, (*4*) fructose-bisphosphate aldolase (*fbaB*), (*5*) glycerol channel protein (*glpF*), (*6*) glycerol dehydrogenase (*gldA*): dihydroxyacetone, (*7*) dihydroxyacetone kinase (*dhaKLM*), (*8*) triosephosphate isomerase (*tpiA*): glyceraldehyde-3-P, (*9*) glyceraldehyde-3-phosphate dehydrogenase A (*gapA*): 1,3-bisphosphoglycerate, (*10*) phosphoglycerate kinase (*pgk*): 3-phosphoglycerate, (*11*) phosphoglyceromutase 1 (*gpmA*):2-phosphoglycerate, (*12*) enolase (*eno*), (*13*) pyruvate kinase I/II (*pykFA*), (*14*) phosphoenolpyruvate carboxylase (*pepC*): oxaloacetate, (*15*) malate dehydrogenase (*mdh*): malate, (*16*) fumarase A, B, and C (*fumABC*): fumarate, (*17*) fumarate reductase (*frdABCD*), (*18*) succinyl-CoA synthetase (*sucCD*): succinyl-CoA, (*19*) methylmalonyl-CoA mutase (*scpA*): L-methylmalonyl-CoA, (*20*) methylmalonyl-CoA decarboxylase (*scpB*): propionyl-CoA, (*21*) propionyl-CoA/succinate CoA transferase (*scpC*): succinyl-CoA and propionate, (*22*) alcohol dehydrogenase (*adhE*): propionaldehyde, (*23*) alcohol dehydrogenase (*adhE*), (*24*) methylglyoxal synthase (*mgsA*): methylglyoxal, (*25*) methylglyoxal reductase (*mgr*): L-lactaldehyde, (*26*) glyoxalase I (*gloA*): *S*-lactoyl-glutathione, (*27*) glyoxalase III (*hchA*), (*28*) lactaldehyde dehydrogenase (*aldA*), (*29*) *S*-lactoylglutathione hydrolase (*yeiG*) and glyoxalase II (*gloB*), (*30*) D-lactate dehydrogenase (*ldhA*), (*31*) pyruvate formate lyase I (*pflB*), (*32*) phosphate acetyltransferase (*pta*), (*33*) acetate kinase A (*ackA*), (*34*) alcohol dehydrogenase (*adhE*): acetaldehyde, (*35*) alcohol dehydrogenase (*adhE*), (*36*) citrate synthase (*gltA*): citrate, (*37*) aconitate hydratase/2-methylisocitrate dehydratase (*acnB*): *cis*-aconitate, (*38*) aconitate hydratase/2-methylisocitrate dehydratase (*acnB*): D-*threo*-isocitrate, (*39*) isocitrate dehydrogenase (*icd*): 2-oxoglutarate. *Green lines* indicate ATP-generating reactions, *red lines* indicate ATP-consuming reactions, *blue lines* indicate NADH-generating reactions, *pink lines* indicate NADH-consuming reactions, and *orange lines* indicate NADPH-consuming reactions. *Compounds highlighted in blue* represent primary carbon sources, *compounds highlighted in green* represent target solvents, and *compounds highlighted in red* represent undesirable metabolites. *Wavy lines* represent intermediate reactions of the PTS for glucose and glycerol metabolism. **b** Overall reactions (r_1–r_{10}) connecting major metabolic nodes. Theoretical yields are calculated based on stoichiometric ratio of the product to the initial substrate (i.e., glucose or glycerol)

Materials and methods

Bacterial strains and plasmids

E. coli strains, plasmids, and DNA primers used in this study are listed in Table 1. Standard recombinant DNA technologies for molecular cloning were applied (Miller 1992). *Pfu* and *Taq*

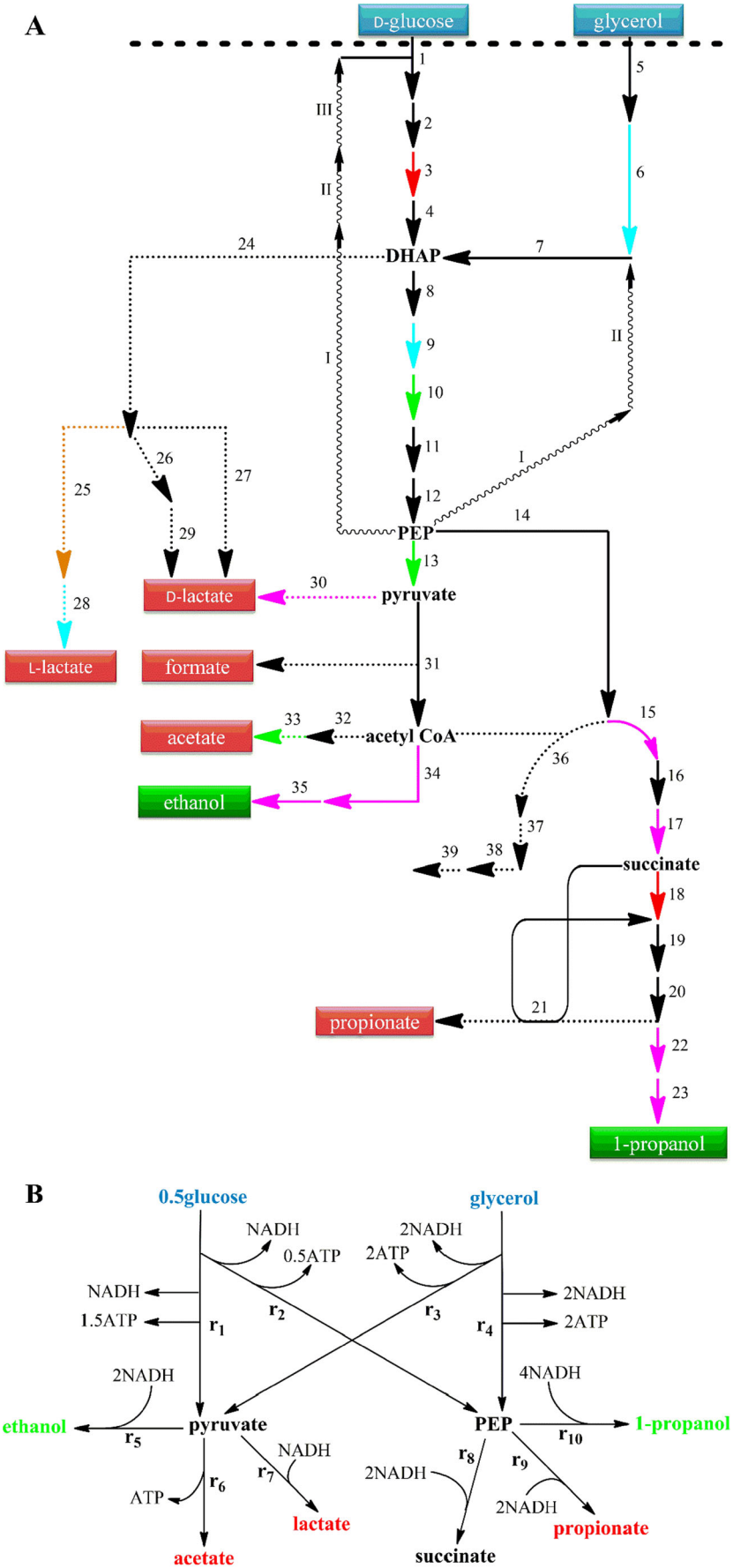
A
D-glucose
glycerol
DHAP
PEP
pyruvate
acetyl CoA
D-lactate
L-lactate
formate
acetate
ethanol
propionate
succinate
1-propanol
B
0.5glucose
glycerol
NADH
0.5ATP
2NADH
2ATP
1.5ATP
4NADH
ethanol
pyruvate
PEP
1-propanol
lactate
ATP
acetate
succinate
propionate

Table 1 List of *E. coli* strains, plasmids, and primers used in this study

Name	Description, relevant genotype or primer sequence (5′→3′)	Reference
E. coli host strains		
HST08	F-, *endA1*, *supE44*, *thi-1*, *recA1*, *relA1*, *gyrA96*, *phoA*, *Φ80d lacZΔ M15*, Δ(*lacZYA–argF*) *U169*, Δ(*mrr–hsdRMS–mcrBC*), *ΔmcrA*, λ–	TaKaRa Bio Inc.
MC4100	F-, [*araD139*]B/r, Del(*argF-lac*)169, λ–, e14-, *flhD5301*, Δ(*fruK-yeiR*)*725*(*fruA25*), *relA1*, *rpsL150*(strR), *rbsR22*, Del(*fimB-fimE*)*632*(::IS1), *deoC1*	Casadaban 1976 (CGSC#: 6152)
BW25141	F-, Δ(*araD-araB*)567, Δ*lacZ4787*(::*rrnB-3*), Δ(*phoB-phoR*)*580*, λ-, *galU95*, Δ*uidA3*::pir+, *recA1*, *endA9*(del-ins)::FRT, *rph-1*, Δ(*rhaD-rhaB*)*568*, *hsdR514*	Datsenko and Wanner 2000 (CGSC#: 7635)
BW25113	F-, Δ(*araD-araB*)*567*, Δ*lacZ4787*(::*rrnB-3*), λ-, *rph-1*, Δ(*rhaD-rhaB*)*568*, *hsdR514*	Datsenko and Wanner 2000 (CGSC#: 7636)
WT-Δ*ldhA*	*ldhA* null mutant of BW25113	Srirangan et al. 2013
WT-Δ*ldhA*-Δ*pykF*	*ldhA*/*pykF* double null mutant of BW25113	This study
CPC-CNTRL1	BW25141/pK184	This study
CPC-CNTRL2	WT-Δ*ldhA*/pK184	This study
CPC-PrOH1	BW25141/pK-scpAKB	This study
CPC-PrOH2	WT-Δ*ldhA*/pK-scpAKB	This study
CPC-PrOH3	WT-Δ*ldhA*-Δ*pykF*, P_{trc}::*sbm* (i.e., with the FRT-CmR-FRT-P_{trc} cassette replacing the 204-bp upstream of the Sbm operon)	This study
Plasmids		
pCP20	FLP^+, λ $cI857^+$, λ p_R Rep(pSC101 ori)^{ts}, Ap^R,Cm^R	Cherepanov and Wackernagel 1995
pKD46	$RepA101^{ts}$ ori, Ap^R, *araC*-P_{araB}:*gam-bet-exo*	Datsenko and Wanner 2000
pTrc99a	ColE1 ori, Ap^R, P_{trc}	Amann et al. 1988
pKD3	R6K-γ ori, Ap^R, FRT-Cm^R-FRT	Datsenko and Wanner 2000
pK184	p15A ori, Km^R, P_{lac}:*lacZ*'	Jobling and Holmes 1990
pK-scpAKB	From pK184, P_{lac}:*sbm-ygfD-ygfG*	Srirangan et al. 2013
Primers		
v-ldhA	TCATCAGCAGCGTCAACGGC; ATCGCTGGTCACGGGCTTACCGTT	Srirangan et al. 2013
v-pykF	TAGCAATTGAGCGATGATATATTTATACACCGG; TCGTTGCTCAGCTGGTCAACTTT	This study
c-frt	AGATTGCAGCATTACACGTCTTGAG; CCAGCTGCATTAATGAATCGGGCCATGGTC CATATGAATATCCTCC	This study
c-ptrc	CCGATTCATTAATGCAGCTGG; GGTCTGTTTCCTGTGTGAAATTGTTA	This study
r-frt:ptrc	CTCGATTATGGTCACAAAGTCCTTCGTCAGGATTAAAGATTGCAGCATTACACGTCTT GA; GTTGGCAAGCTGTTGCCACTCCTGCACGTTAGACATGGTCTGTTTCCTGTGTGA AATTGT	This study
v-frt:ptrc	GCGCTCGACTATCTGTTCGTCAGCTC; TCGACAGTTTTCTCCCGACGGCTCA	This study

Underlined sequences within the primers denote the homology arms (H1 and H2)

v verification primer, *r* recombineering primer, *c* cloning primer

DNA polymerases, T4 DNA ligase, and large (Klenow) fragment of DNA Polymerase I were obtained from New England Biolabs (Ipswich, MA). All synthesized oligonucleotides were obtained from Integrated DNA Technologies (Coralville, IA). DNA sequencing was conducted by the Centre for Applied Genomics at the Hospital for Sick Children (Toronto, Canada).

E. coli BW25141 was used to provide the parental genetic background for 1-propanol production. *E. coli* HST08 was used for molecular cloning. Gene knockouts were introduced to BW25141 strains by P1-phage transduction (Miller 1992) using proper Keio Collection strains (The Coli Genetic Stock Center, Yale University) as donors (Baba et al. 2006). The co-transduced Km^R-FRT gene cassette was removed using pCP20 (Datsenko and Wanner 2000). The genotypes of derived knockout strains were confirmed by colony PCR using appropriate primer sets.

To fuse the strong promoter (P_{trc}) with the Sbm operon in the *E. coli* genome, we used a modified λ Red-mediated recombination protocol (Sukhija et al. 2012) (Fig. 2). The FRT-Cm^R-FRT cassette was PCR-amplified from pKD3 using the c-frt primer set, whereas the P_{trc} promoter-operator fragment was PCR-amplified from pTrc99a using the c-ptrc primer set. The two DNA fragments were fused by splice overlap extension (SOE) PCR (Barnard 2005) using the forward primer of the c-frt primer set and the reverse primer of the c-ptrc primer set to generate the FRT-Cm^R-FRT-P_{trc} cassette. To generate the DNA cartridge for genomic integration, the FRT-Cm^R-FRT-P_{trc} cassette was PCR-amplified using the r-frt:ptrc primer set containing the 36-bp homology arms of H1 and H2, respectively. To derive the plasmid-free strain of CPC-PrOH3, 0.5 μg of the amplified/purified DNA cassette was electrotransformed, using a Gene Pulser (Bio-Rad Laboratories, Hercules, CA) set at 2.5 kV, 25 μF, and 200 Ω, to WT-Δ*ldhA*-Δ*pykF* harboring the λ-Red recombinase expression plasmid pKD46 for DNA recombination to replace the 204-bp upstream region of the Sbm operon (Fig. 2). Expression of the λ-Red recombination enzymes and preparation of competent cells were carried out as described by Datsenko and Wanner (2000). After electroporation, cells were resuspended in 500 μL of SOC (super optimal broth with catabolite repression) medium (3.6 g/L glucose, 20 g/L tryptone, 5 g/L yeast extract, 0.6 g/L NaCl, 0.19 g/L KCI, 4.8 g/L $MgSO_4$) (Hanahan 1983) and recuperated at 37 °C for 1 h in a rotatory shaker at 250 rpm (New Brunswick Scientific, NJ). Cells were then plated on lysogeny broth (LB) agar containing 12 μg/mL chloramphenicol for incubation at 37 °C for 16 h to select chloramphenicol-resistant recombinants. The fusion of the FRT-Cm^R-FRT-P_{trc} cassette with the Sbm operon was verified by colony PCR using the v-frt:ptrc primer set as well as DNA sequencing.

Media and cultivation conditions

All media components were obtained from Sigma-Aldrich Co. (St Louis, MO) except glucose, yeast extract, and tryptone which were obtained from BD Diagnostic Systems (Franklin Lakes, NJ). Media was supplemented with antibiotics as required (30 μg/mL kanamycin and 12 μg/mL chloramphenicol). For 1-propanol production, propanogenic *E. coli* strains (stored as glycerol stocks at −80 °C) were streaked on LB agar plates with appropriate antibiotics and incubated at 37 °C for 16 h. Single colonies were picked from LB plates to inoculate 30 mL SB medium (32 g/L tryptone, 20 g/L yeast extract, and 5 g/L NaCl) with appropriate antibiotics in 125-mL conical flasks. Overnight cultures were shaken at 37 °C and 280 rpm in a rotary shaker (New Brunswick Scientific, NJ) and used as seed cultures to inoculate 200 mL SB media at 1 % (*v*/*v*) with appropriate antibiotics in 1-L conical flasks. This second seed culture was shaken at 37 °C and 280 rpm for approximately 16 h. Cells were then harvested by centrifugation at 6000×*g* and 20 °C for 15 min and resuspended in 100-mL fresh LB media. The suspended culture was used to inoculate a 1-L stirred-tank bioreactor (Omni-Culture, VirTis, NY) operated anaerobically at 30 °C and 430 rpm. The production medium in the bioreactor contained 30 g/L carbon

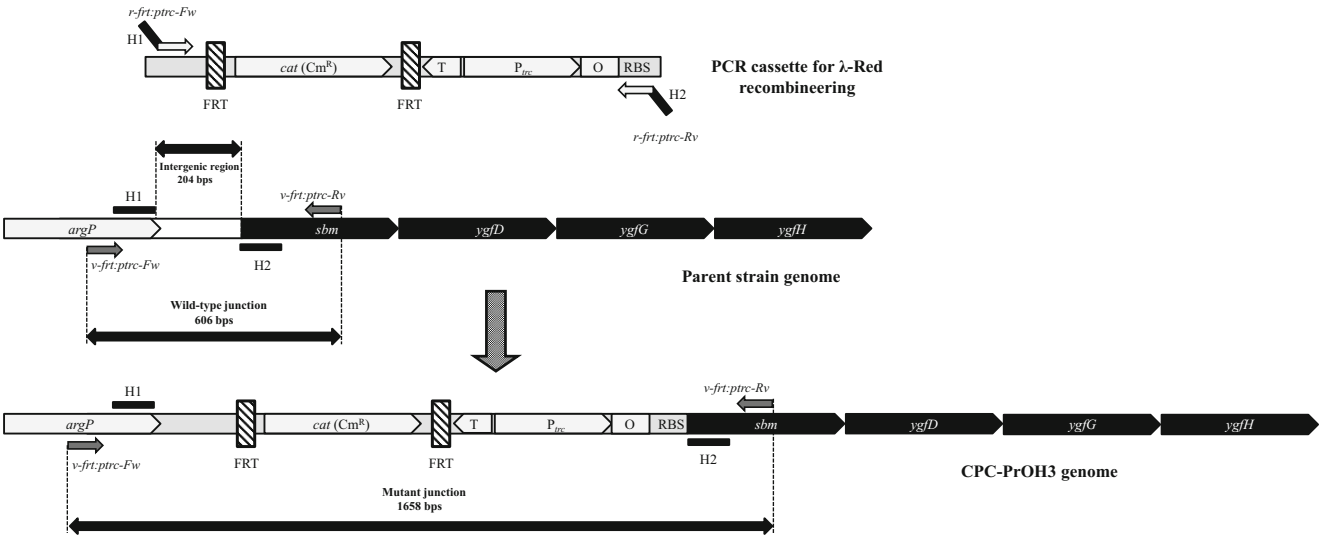

Fig. 2 Genomic engineering for deriving the plasmid-free propanogenic strain CPC-PrOH3. In order to activate the naturally silent Sbm operon with the strong promoter (P_{trc}), the FRT-CmR-FRT-P_{trc} fragment was PCR-amplified using the primer set of r-frt:ptrc with homology extensions (*H1* and *H2*) for λ-Red-mediated recombination to replace the superfluous 204-bp region upstream of the operon. The primer set of r-frt:ptrc was used to PCR-verify the genotype of CPC-PrOH3. Genes and regulatory elements [i.e., operator (*O*), terminator (*T*) and ribosome binding site (*RBS*)] are not to scale

source (i.e., glucose or glycerol), 0.23 g/L K_2HPO_4, 0.51 g/L NH_4Cl, 49.8 mg/L $MgCl_2$, 48.1 mg/L K_2SO_4, 1.52 mg/L $FeSO_4$, 0.055 mg/L $CaCl_2$, 2.93 g/L NaCl, 0.72 g/L tricine, 10 g/L yeast extract, 10 mM $NaHCO_3$, 0.2 μM cyanocobalamin (vitamin B_{12}), trace elements (2.86 mg/L H_3BO_3, 1.81 mg/L $MnCl_2{\cdot}4H_2O$, 0.222 mg/L $ZnSO_4{\cdot}7H_2O$, 0.39 mg/L $Na_2MoO_4{\cdot}2H_2O$, 79 μg/L $CuSO_4{\cdot}5H_2O$, 49.4 μg/L $Co(NO_3)_2{\cdot}6H_2O$), and appropriate antibiotics (Neidhardt et al. 1974). Anaerobic conditions were maintained by constant bubbling of nitrogen. The pH of the production culture was maintained at 7.0±0.1 with 30 % (*v*/*v*) NH_4OH and 15 % (*v*/*v*) HNO_3. The feeding solution for fed-batch cultivation contained 500 g/L glycerol only and 50 mL of it was added manually when the glycerol concentration in the production culture fell below 5 g/L. Note that no isopropyl β-D-1-thiogalactopyranoside (IPTG) was supplemented in the cultivation medium for induction purposes since it was observed that IPTG supplementation had negligible effects on the 1-propanol production for all propanogenic strains in this study.

Analyses

Culture samples were appropriately diluted with saline for measuring the optical cell density (OD_{600}) using a spectrophotometer (DU520, Beckman Coulter, Fullerton, CA). Cell-free supernatant was collected and filter sterilized for titer analysis of glucose, glycerol, and various metabolites using an HPLC (LC-10AT, Shimadzu, Kyoto, Japan) with a refractive index detector (RID-10A, Shimadzu, Kyoto, Japan) and a chromatographic column (Aminex HPX-87H, Bio-Rad Laboratories, CA, USA). The column temperature was maintained at 65 °C and the mobile phase was 5 mM H_2SO_4 (pH 2.0) running at 0.6 mL/min. The RID signal was acquired and processed by a data processing unit (Clarity Lite, DataApex, Prague, Czech Republic).

Results

Biosynthesis of 1-propanol using engineered *E. coli* strains

Anaerobic cultivation of the propanogenic strain CPC-PrOH1 was conducted in a bioreactor using glucose as the major carbon source for the production of 1-propanol (Fig. 3b). The control strain CPC-CNTRL1, harboring an inactive Sbm operon on the genome, had a similar glucose dissimilation pattern to CPC-PrOH1 in terms of cell growth and metabolite production, but showed elevated succinate levels and no 1-propanol production (Fig. 3a). Introducing the Sbm operon genes (i.e., *sbm-ygfD-ygfG*) for episomal expression made the *E. coli* strain propanogenic with a reduced level of succinate, implying 1-propanol was produced through extensive dissimilation of succinate via the Sbm pathway (Fig. 1a). Nevertheless, 1-propanol titer reached only 0.11 g/L with lactate, acetate, and ethanol being the major metabolites (Fig. 3b). Note that previously, in addition to the Sbm operon, two other genes, i.e., *sucCD* (encoding succinyl-CoA synthetase) and *adhE* (encoding the bifunctional aldehyde/alcohol dehydrogenase), were coexpressed episomally to alleviate potential limitation of these conversion steps (Srirangan et al. 2013). However, the resulting strains suffered a significant physiological burden associated with the maintenance of multiple plasmids and, consequently, 1-propanol productivity was limited. The physiological limitation appeared minimal for the single-plasmid system of CPC-PrOH1, implying that the aldehyde/alcohol dehydrogenase from *E. coli* was effective in driving 1-propanol production. While glucose dissimilation was complete within 14 h, anaerobic fermentation appeared to significantly lean toward acidogenesis rather than solventogenesis. More than 80 % of dissimilated glucose was converted to acetate, lactate, and succinate (Fig. 3), with lactate accounting for more than 60 %. On the other hand, only ~15 % was diverted to solventogenesis for ethanol and 1-propanol production. It should be noted that formate was not detected in any of the cultures, likely due to active formate dehydrogenases which oxidizes this endogenously produced metabolite into CO_2.

Since lactate was significantly overproduced, the *ldhA* gene (encoding lactate dehydrogenase) was inactivated with the intention of reducing lactate accumulation as well as shifting carbon flux toward solventogenesis. Culture performance of this mutant strain with glucose as the major carbon source and metabolite profiling are summarized in Fig. 4. Similar to the strains with the parental genetic background, the control *ldhA* mutant strain CPC-CNTRL2 with an inactive Sbm operon on the genome produced elevated levels of succinate (Fig. 4a), whereas the *ldhA* mutant strain CPC-PrOH2 with episomal Sbm expression for extended dissimilation of succinate became propanogenic (Fig. 4b). The efficiency of glucose dissimilation was slightly affected by *ldhA* disruption as total consumption occurred within 18 h of cultivation. Notably, lactate levels of the *ldhA* mutant strains were significantly

Fig. 3 Time profiles of glucose, biomass, and major metabolites during batch cultivation of **a** CPC-CNTRL1 and **b** CPC-PrOH1 with glucose as the major carbon source. Culture performance (i.e., overall glucose consumption and final biomass and metabolite concentrations) of batch cultivation in a bioreactor is summarized in the tables below each time profile. The glucose equivalent for each metabolite is calculated based on the corresponding theoretical yield in Fig. 1b. The metabolite distribution (i.e., the fraction of dissimilated glucose to form a metabolite) is defined as the ratio of the glucose equivalent of a metabolite to the sum of the total glucose equivalents of all metabolites

A

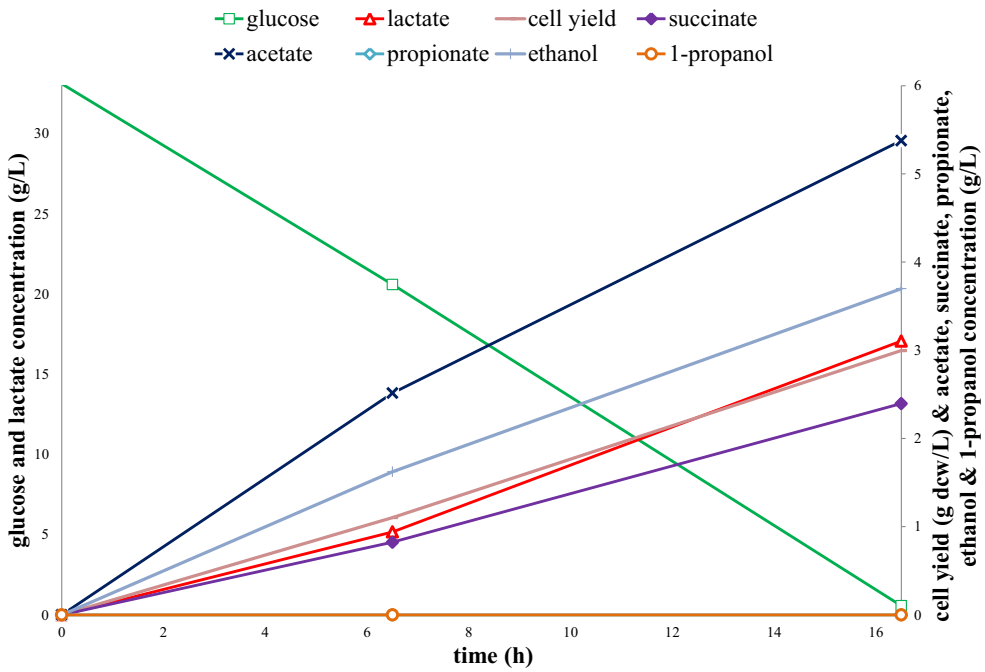

	Glucose	Biomass	Succinate	Lactate	Acetate	Propionate	Ethanol	1-Propanol
Concentration[a] (g/L)	32.55	3.00	2.40	17.08	5.38	ND	3.73	ND
Glucose equivalent[b] (g/L)	-	-	1.83	17.08	8.20	-	7.29	-
Metabolite distribution[c] (%)	-	-	5.31	49.62	23.82	-	21.19	-

B

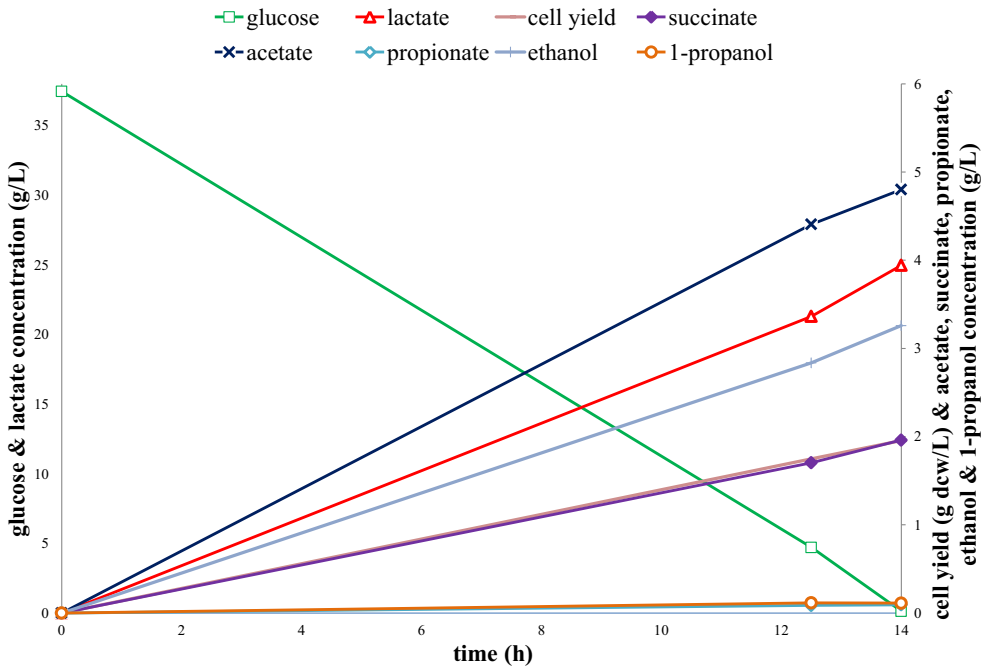

	Glucose	Biomass	Succinate	Lactate	Acetate	Propionate	Ethanol	1-Propanol
Concentration[a] (g/L)	37.32	1.96	1.96	24.97	4.80	0.09	3.26	0.11
Glucose equivalent[b] (g/L)	-	-	1.50	24.97	7.32	0.11	6.38	0.17
Metabolite distribution[c] (%)	-	-	3.70	61.73	18.10	0.28	15.77	0.42

[a] initial glucose concentration, biomass concentration (g-DCW/L), and major metabolite concentrations
[b] calculated based on theoretical yield of each metabolite to glucose (Fig. 1b)
[c] represents the fraction of assimilated glucose

reduced to 2 g/L, representing a ~90 % reduction compared to the control strains. Low concentrations of lactate were still detected in the cultures of the *ldhA* mutant strains and these small amounts of lactate can be associated with alternative lactate synthetic routes such as the methylglyoxal pathway (Fig. 1) (Jantama et al. 2008). Carbon flux was redirected toward acetate overproduction and enhanced solventogenesis, with acetate and ethanol titers accounting for 47 and 34 % of dissimilated glucose, respectively, during CPC-PrOH2 cultivation (Fig. 4b). Most importantly, the 1-propanol titer of the CPC-PrOH2 culture increased significantly to 0.55 g/L, corresponding to five-fold that of the CPC-PrOH1 culture.

Glycerol serves as a superior carbon source for enhanced solventogenesis

Glycerol is a potentially superior carbon source to glucose, particularly for biofuel production, due to its higher reductance, leading to higher biomass yields and less acidogenesis during fermentation (da Silva et al. 2009). Recent oversupply in the biodiesel industry has made glycerol, a by-product of biodiesel production, an economically viable feedstock for biomanufacturing (Clomburg and Gonzalez 2011). Accordingly, glycerol was investigated as a carbon source for anaerobic cultivation of the *ldhA* mutant propanogenic strain, CPC-PrOH2, for 1-propanol production (Fig. 5). Compared with glucose, the glycerol dissimilation rate of CPC-PrOH2 was much slower during batch cultivation, requiring more than 80 h to consume 30 g of glycerol whereas 18 h to consume 30 g of glucose. However, high ethanol titers of 10.9 and 9.3 g/L were obtained for CPC-CNTRL2 and CPC-PrOH2, respectively, when glycerol was used as the major carbon source. Most importantly, 1-propanol titer was 2.15 g/L for CPC-PrOH2, representing an approximate four-fold increase compared to the batch culture of CPC-PrOH2 with glucose as the major carbon source. The results show that more than 70 % of glycerol dissimilation was directed toward solventogenesis (Fig. 5). In contrast to cultures with glucose as the major carbon source, acetate production was minimal and lactate was even undetectable when glycerol was used. This can alleviate the physiological impacts associated with the presence of organic acids in *E. coli* cultures (van de Walle and Shiloach 1998), which may limit 1-propanol production. Note that the control strain CPC-CNTRL2 accumulated succinate to 3.45 g/L, whereas the succinate concentration was merely 0.62 g/L for CPC-PrOH2 (Fig. 5), implying that the extended dissimilation of succinate via episomal expression of the Sbm operon was functional. In addition, glycerol dissimilation appeared more effective upon episomal expression of the Sbm operon since it took 134 and 85 h to consume 30 g glycerol for CPC-CNTRL2 and CPC-PrOH2, respectively.

Fig. 4 Time profiles of glucose, biomass, and major metabolites during batch cultivation of **a** CPC-CNTRL2 and **b** CPC-PrOH2 with glucose as the major carbon source. Culture performance (i.e., overall glucose consumption and final biomass and metabolite concentrations) of batch cultivation in a bioreactor is summarized in the tables below each time profile. The glucose equivalent for each metabolite is calculated based on the corresponding theoretical yield in Fig. 1b. The metabolite distribution (i.e., the fraction of dissimilated glucose to form a metabolite) is defined as the ratio of the glucose equivalent of a metabolite to the sum of the total glucose equivalents of all metabolites

Fed-batch cultivation for high-level coproduction of 1-propanol and ethanol

To extend 1-propanol productivity, fed-batch cultivation of CPC-PrOH2 was explored using glycerol as the major carbon source (Fig. 6 and Table 2). Unlike fed-batch cultures using glucose as the major carbon source where a specific glucose feeding profile must be developed to prevent the overaccumulation of organic acids impacting culture performance (Korz et al. 1995), no glycerol feeding profile was required due to minimal acidogenesis associated with glycerol dissimilation. Instead, a designated amount of glycerol was intermittently fed into the culture as a single inoculum to increase glycerol concentration to 20–25 g/L when depletion of glycerol was observed. The fed-batch culture of CPC-PrOH2 was divided into four stages with glycerol being fed at the start of each stage (Fig. 6) and metabolic analysis was conducted for each stage (Table 2). More than 70 % of glycerol dissimilation was directed toward solventogenesis, with ethanol and 1-propanol being the two major metabolites, and such high-level solventogenesis was maintained toward the end of the fed-batch culture (Table 2). This led to high-level coproduction of ethanol at 25 g/L and 1-propanol at 3.78 g/L. Note that these titers were underestimated due to the dilution by fed glycerol. Given the persistence of high-level solventogenesis throughout the entire fed-batch cultivation, 1-propanol yield steadily decreased and hardly any 1-propanol was produced during the last stage. The results suggest the deterioration of the bioactivity of the Sbm operon, which also resulted in the accumulation of succinate to a high level of 5.44 g/L at the end of the fed-batch cultivation. Glycerol dissimilation rate was increased by approximately 30 % upon fed-batch operation (i.e., from 0.35 g/L/h in Stage I to approximately 0.45 g/L/h afterwards) (Fig. 6), presumably due to an increased biomass concentration. While the level of acidogenesis remained low during the entire fed-batch cultivation, acetate steadily accumulated to a final concentration of 8.15 g/L which could potentially impact culture performance. The deterioration in culture performance can also be observed by the decreasing efficiency of glycerol utilization toward metabolite production (Table 2),

A

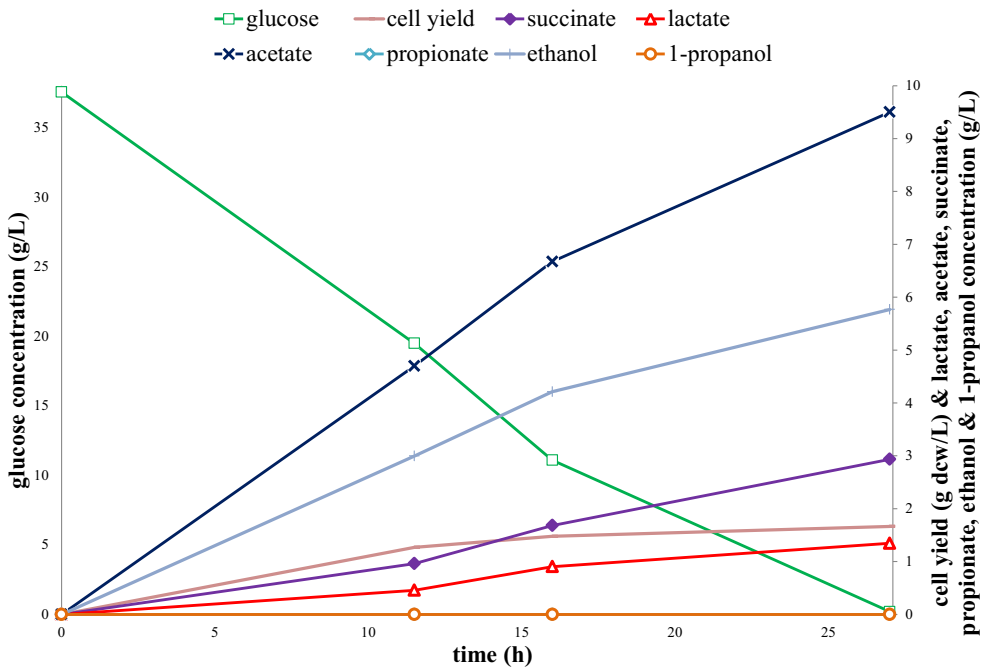

	Glucose	Biomass	Succinate	Lactate	Acetate	Propionate	Ethanol	1-Propanol
Concentration[a] (g/L)	37.35	1.67	2.94	1.35	9.50	ND	5.77	ND
Glucose equivalent[b] (g/L)	-	-	2.24	1.36	14.82	-	11.54	-
Metabolite distribution[c] (%)	-	-	7.62	4.63	49.31	-	38.43	-

B

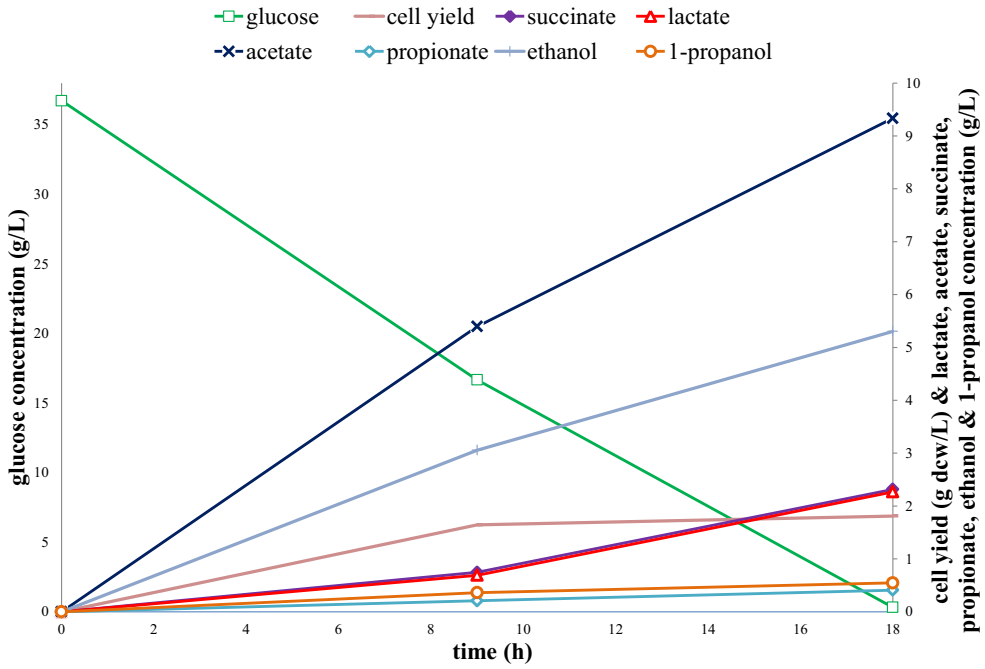

	Glucose	Biomass	Succinate	Lactate	Acetate	Propionate	Ethanol	1-Propanol
Concentration[a] (g/L)	36.41	1.81	2.32	2.27	9.33	0.41	5.31	0.55
Glucose equivalent[b] (g/L)	-	-	1.77	2.29	14.23	0.50	10.38	0.82
Metabolite distribution[c] (%)	-	-	5.89	7.65	47.45	1.66	34.62	2.73

[a] initial glucose concentration, biomass concentration (g-DCW/L), and major metabolite concentrations
[b] calculated based on theoretical yield of each metabolite to glucose (Fig. 1b)
[c] represents the fraction of assimilated glucose

suggesting that a certain amount of glycerol was consumed for cell maintenance and sustained viability in increasingly harsh cultivation conditions during the late stages of fed-batch cultivation.

Derivation of plasmid-free propanogenic ***E. coli*** strains

It has been well perceived that plasmid-free strains outperform recombinant ones in metabolite production for which gene dosage seldom limits the yield of the target metabolite (Jones et al. 2000). Since wild-type *E. coli* has the silent Sbm operon potentially due to an inactive promoter, plasmid-free propanogenic *E. coli* strains were derived by replacing the 204-bp intergenic region upstream of the chromosomal Sbm operon with a strong *trc*-promoter (P_{trc}) using our previously developed protocol for genomic engineering (Sukhija et al. 2012). A chloramphenicol-resistance cassette flanked by two FRT sites was fused with a P_{trc} promoter-operator fragment via Splicing by Overlap Extension (SOE)-PCR. The DNA fusion (FRT-Cm^R-FRT- P_{trc}) was then used to replace the region upstream of the native Sbm operon on the genome to form the engineered strain CPC-PrOH3 (Fig. 2). The 1-propanol production capacity of the plasmid-free strain CPC-PrOH3 was characterized using fed-batch cultivation with glycerol as the major carbon source (Fig. 7 and Table 2). While the levels of solventogenesis for CPC-PrOH3 and CPC-PrOH2 were similar during Stage I for batch cultivation (i.e., the sum of ethanol and 1-propanol titers was approximately equivalent to 74 % of dissimilated glycerol for both strains) (Table 2), the glycerol dissimilation rate for CPC-PrOH3 was approximately two-fold that for CPC-PrOH2 since it took 42.5 h (Fig. 7) and 85.5 h (Fig. 6) for CPC-PrOH3 and CPC-PrOH2, respectively, to consume 30 g/L glycerol during Stage I. In addition to the higher glycerol dissimilation rate, CPC-PrOH3 produced slightly more 1-propanol than CPC-PrOH2 (2.44 versus 2.15 g/L) during Stage I. Moreover, unlike CPC-PrOH2 which exhibited a low glycerol dissimilation rate and steadily deteriorating 1-propanol yield, the high glycerol dissimilation rate and high 1-propanol yield of CPC-PrOH3 in Stage I (equivalent to 12–13 % of dissimilated glycerol) even persisted during Stage II and III of fed-batch cultivation (Table 2). The results suggest that a single chromosomal copy of the active Sbm operon was sufficient to drive 1-propanol production without metabolic burden and physiological impact associated with the active Sbm operon located in a multicopy plasmid. Using CPC-PrOH3 for fed-batch cultivation with glycerol as the major carbon source, the 1-propanol titer soared to 6.76 g/L. The final ethanol titer also reached a high level of 31.1 g/L which is equivalent to approximately 70 % of dissimilated glycerol. Similar to the CPC-PrOH2 fed-batch culture, while the level of acidogenesis remained low during the entire fed-batch cultivation of CPC-PrOH3, acetate steadily accumulated to a final concentration of 9.41 g/L which could potentially impact

Fig. 5 Time profiles of glycerol, biomass, and major metabolites during batch cultivation of **a** CPC-CNTRL2 and **b** CPC-PrOH2 with glycerol as the major carbon source. Culture performance (i.e., overall glycerol consumption and final biomass and metabolite concentrations) of batch cultivation in a bioreactor is summarized in the tables below each time profile. The glycerol equivalent for each metabolite is calculated based on the corresponding theoretical yield in Fig. 1b. The metabolite distribution (i.e., the fraction of dissimilated glycerol to form a metabolite) is defined as the ratio of the glycerol equivalent of a metabolite to the sum of the total glucose equivalents of all metabolites

culture performance. However, the final succinate level was only 2.05 g/L for CPC-PrOH3, as opposed to a much higher level of 5.44 g/L for CPC-PrOH2, implying that carbon is more efficiently channeled into the 1-propanol pathway for CPC-PrOH3. Similar to CPC-PrOH2, decreasing efficiency of glycerol utilization for metabolite production can be observed after Stage II of the CPC-PrOH3 fed-batch culture (Table 2), suggesting that metabolic burden could still exist during latter stages.

Discussion

While the production of 1-propanol in *E. coli* was previously achieved through activation of the keto-acid (Atsumi et al. 2008a; Jun Choi et al. 2012; Shen and Liao 2013) or extended 1,2-propanediol (Jain and Yan 2011) pathways, we herein take an alternative approach via extended dissimilation of succinate by activating the endogenous Sbm operon in *E. coli*. Under anaerobic conditions, succinate could accumulate as one of the final fermentation products, although activation of the Sbm operon reduced succinate accumulation as 1-propanol was produced (Figs. 3, 4, and 5). Nevertheless, 1-propanol production appeared to be highly dependent on culture conditions, particularly carbon source. The use of glucose as the major carbon source resulted in dominance of acidogenesis over solventogenesis with low yields of 1-propanol. Further inspection of the major active pathways during glucose fermentation reveals inherent constraints of the metabolic network that prevent sufficient diversion of carbon flux from the phosphoenolpyruvate (PEP) node toward the reductive arm of oxaloacetate for 1-propanol biosynthesis. The metabolic deficiency is in part due to the high redox demand for 1-propanol production. As illustrated in Fig. 1, PEP generation from glucose produces only one mole of NADH per mole of PEP produced, whereas subsequent 1-propanol production requires four moles of NADH per mole formed. As a result, a large fraction (up to 95 %) of the PEP derived from glucose was channeled into the pyruvate node to prevent such a redox imbalance, forming lactate, acetate, and ethanol as major metabolites. The limitation in the supply of NADH potentially caused the carbon flux to stall at the succinate node, leading to succinate accumulation even when

A

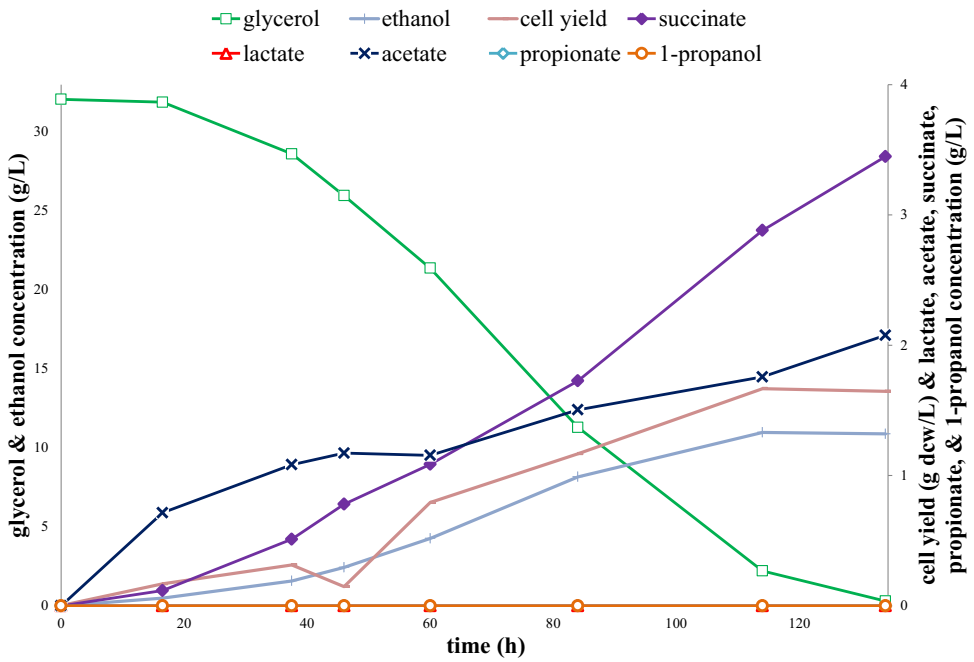

	Glycerol	Biomass	Succinate	Lactate	Acetate	Propionate	Ethanol	1-Propanol
Concentration[a] (g/L)	31.767	1.64	3.45	ND	2.08	ND	10.89	ND
Glycerol equivalent[b] (g/L)	-	-	2.69	-	3.24	-	21.77	-
Metabolite distribution[c] (%)	-	-	9.72	-	11.69	-	78.59	-

B

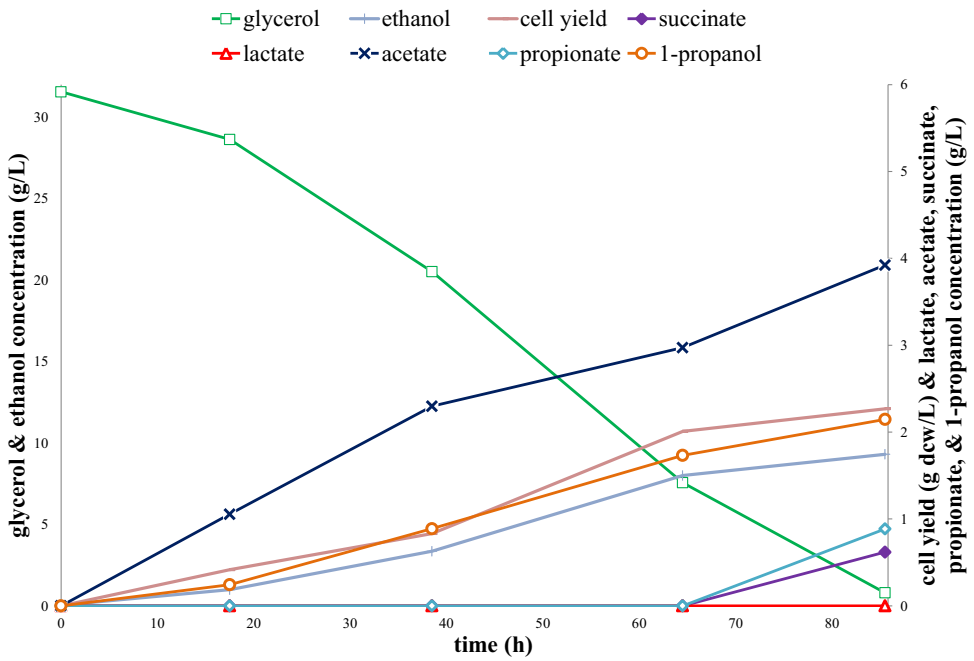

	Glycerol	Biomass	Succinate	Lactate	Acetate	Propionate	Ethanol	1-Propanol
Concentration[a] (g/L)	30.76	2.27	0.62	ND	3.92	0.89	9.31	2.15
Glycerol equivalent[b] (g/L)	-	-	0.47	-	6.12	1.12	18.61	3.30
Metabolite distribution[c] (%)	-	-	1.58	-	20.66	3.77	62.84	11.15

[a] initial glycerol concentration, biomass concentration (g-DCW/L), and major metabolite concentrations
[b] calculated based on theoretical yield of each metabolite to glycerol (Fig. 1b)
[c] represents the fraction of assimilated glycerol
ND not detected

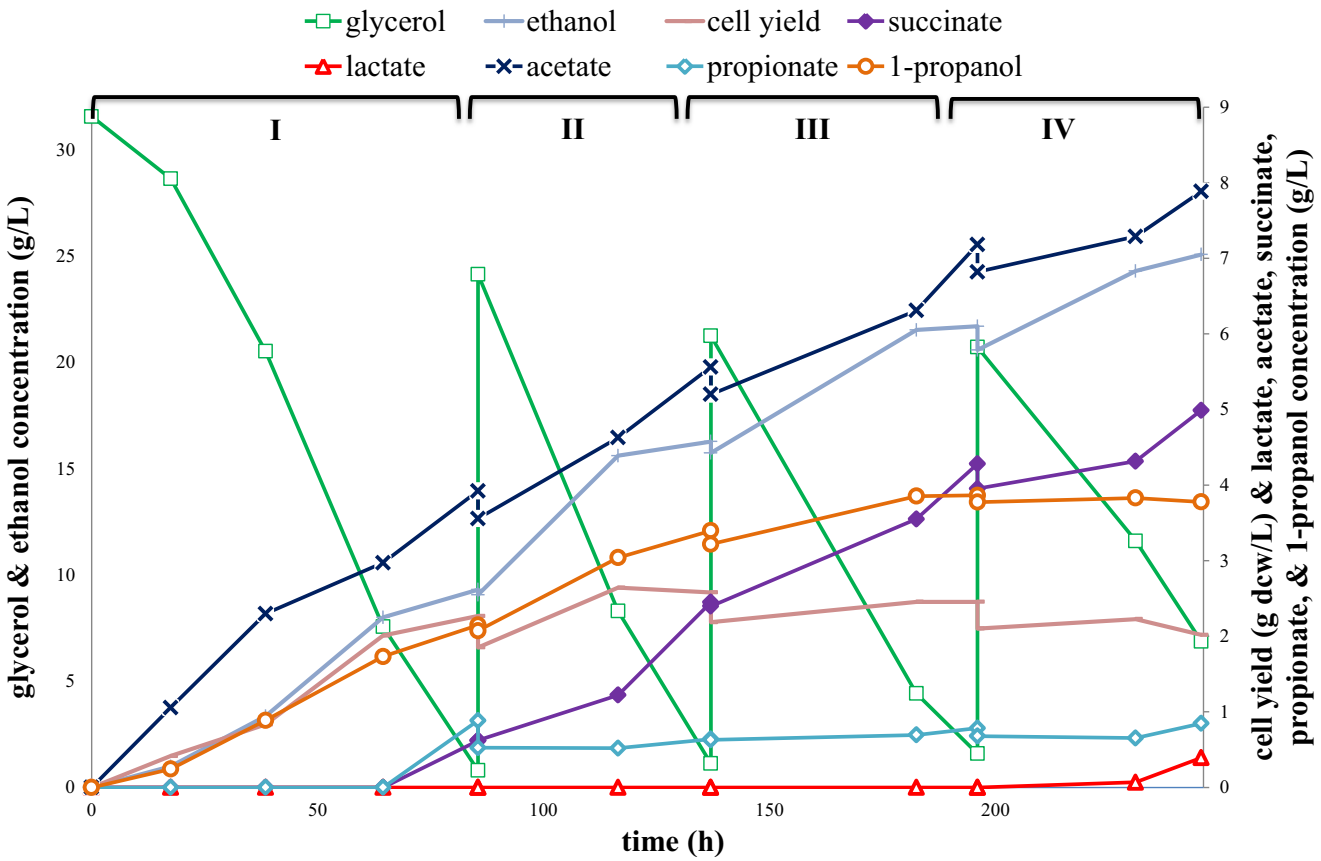

Fig. 6 Time profiles of the concentrations glycerol, biomass, and major metabolites during fed-batch cultivation of CPC-PrOH2 with glycerol as the major carbon source. Approximately 25 g of pure glycerol was fed into the bioreactor in the beginning of each stage and samples were taken before and after the glycerol feeding

the Sbm operon was expressed (Figs. 3b and 4b). For the propanogenic strain CPC-PrOH1 with a parental genetic background, homolactic fermentation dominated, resulting in lactate overproduction and poor 1-propanol yield. Disruption of the major lactate synthesis route by knocking out *ldhA* minimized carbon leakage into the lactate pathway in CPC-PrOH2, but marginally improved 1-propanol production. Upon comparing metabolic profiles for CPC-PrOH1 and CPC-PrOH2 (Figs. 3 and 4), it is evident that the pleiotropic effect associated with the *ldhA* gene knockout was to promote the production of pyruvate-derived fermentative products (i.e., acetate and ethanol), rather than diverting carbon flux to metabolites in the PEP branch, such as succinate and 1-propanol. Nevertheless, the results were unsurprising as similar metabolic effects were previously observed (Srirangan et al. 2013).

Glycerol has obvious advantages over glucose due to a higher reductance and more reducing equivalents generated upon its dissimilation. Nevertheless, glycerol metabolism in *E. coli* is often restricted to respiratory (aerobic) conditions, as the excess reducing equivalents cannot be well consumed by standard redox-balanced pathways in *E. coli* during anaerobiosis (Cintolesi et al. 2012). Accordingly, glycerol appears to be a recalcitrant carbon source in the absence of external electron acceptors for CPC-CNTRL2 (Fig. 5a), whereas an approximately 60 % increase in the glycerol dissimilation rate was observed for the propanogenic strain CPC-PrOH2 (Fig. 5a), suggesting that utilization of the 1-propanol pathway can be an effective means to dispose of excess reducing equivalents generated by glycerol dissimilation. Most importantly, in stark contrast to glucose, the use of glycerol as the major carbon source significantly favored solventogenesis (accounting for up to 84 % of dissimilated glycerol) and minimized acidogenesis, resulting in high-level coproduction of ethanol and 1-propanol. The dramatic switch in the metabolic distribution associated with glycerol fermentation may be in part due to the oxidized nature of metabolites. Incidentally, previous studies reported that *E. coli* produces 1,2-propanediol to attain redox balance during anaerobic fermentation of glycerol (Clomburg and Gonzalez 2011; Dharmadi et al. 2006). While this compound was not detected in the present study, the solventogenic pathways apparently can act as an auxiliary channel for redox balance upon glycerol dissimilation under anaerobic conditions.

During fed-batch cultivation for 1-propanol production, an increase in the rate of glycerol dissimilation was observed

Table 2 Culture performance (i.e., overall glycerol consumption and final biomass and metabolite concentrations) of fed-batch cultivation in a bioreactor for CPC-PrOH2 and CPC-PrOH3 using glycerol as the major carbon source. The glycerol equivalent for each metabolite is calculated based on the corresponding theoretical yield in Fig. 1b. The metabolite distribution (i.e., the fraction of dissimilated glycerol to form a metabolite) is defined as the ratio of the glycerol equivalent of a metabolite to the sum of the total glucose equivalents of all metabolites

		Glycerol	Biomass	Succinate	Lactate	Acetate	Propionate	Ethanol	1-Propanol
CPC-PrOH2									
Stage I 0–85.5 h	Concentration[a] (g/L)	30.76	2.27	0.62	ND	3.92	0.89	9.31	2.15
	Glycerol equivalent[b] (g/L)	–	–	0.47	–	6.12	1.12	18.61	3.30
	Metabolite distribution[c] (%)	–	–	1.58	–	20.66	3.77	62.84	11.15
	Glycerol efficiency[d] (%)	96.26	–	–	–	–	–	–	–
Stage II 85.5–137 h	Concentration[a] (g/L)	23.01	0.73	1.83	ND	2.01	0.11	7.21	1.32
	Glycerol equivalent[b] (g/L)	–	–	1.62	–	3.13	0.14	14.42	2.03
	Metabolite distribution[c] (%)	–	–	7.59	–	14.65	0.67	67.57	9.51
	Glycerol efficiency[d] (%)	92.74	–	–	–	–	–	–	–
Stage III 137–196 h	Concentration[a] (g/L)	19.65	0.27	1.88	ND	1.98	0.16	5.96	0.65
	Glycerol equivalent[b] (g/L)	–	–	1.47	–	3.09	0.20	11.92	0.99
	Metabolite distribution[c] (%)	–	–	8.32	–	17.49	1.11	67.47	5.62
	Glycerol efficiency[d] (%)	89.92	–	–	–	–	–	–	–
Stage IV 196–245.5 h	Concentration[a] (g/L)	13.84	−0.08	1.04	0.39	1.07	0.17	4.49	0.00
	Glycerol equivalent[b] (g/L)	–	–	0.81	0.40	1.66	0.21	8.98	0.01
	Metabolite distribution[c] (%)	–	–	6.70	3.29	13.77	1.76	74.40	0.05
	Glycerol efficiency[d] (%)	87.21	–	–	–	–	–	–	–
CPC-PrOH3									
Stage I 0–42.5 h	Concentration[a] (g/L)	30.73	2.79	0.59	ND	4.04	0.78	9.51	2.44
	Glycerol equivalent[b] (g/L)	–	–	0.46	–	6.30	0.99	19.03	3.75
	Metabolite distribution[c] (%)	–	–	1.51	–	20.64	3.23	62.34	12.29
	Glycerol efficiency[d] (%)	99.34	–	–	–	–	–	–	–
Stage II 42.5–72 h	Concentration[a] (g/L)	22.69	0.38	0.34	ND	1.84	0.37	8.57	2.01
	Glycerol equivalent[b] (g/L)	–	–	0.26	–	2.88	0.46	17.15	3.09
	Metabolite distribution[c] (%)	–	–	1.10	–	12.06	1.94	71.94	12.95
	Glycerol efficiency[d] (%)	105.06	–	–	–	–	–	–	–
Stage III 72–94 h	Concentration[a] (g/L)	18.51	0.65	0.30	ND	1.38	0.12	5.68	1.45
	Glycerol equivalent[b] (g/L)	–	–	0.24	–	2.15	0.16	11.36	2.23
	Metabolite distribution[c] (%)	–	–	1.46	–	13.31	0.96	70.43	13.84
	Glycerol efficiency[d] (%)	87.16	–	–	–	–	–	–	–
Stage IV 94–144 h	Concentration[a] (g/L)	25.67	0.10	0.85	ND	2.39	0.17	7.33	1.07
	Glycerol equivalent[b] (g/L)	–	–	0.66	–	3.73	0.21	14.65	1.65
	Metabolite distribution[c] (%)	–	–	3.16	–	17.86	1.00	70.08	7.90
	Glycerol efficiency[d] (%)	81.41	–	–	–	–	–	–	–
Stage V 144–210.5 h	Concentration[a] (g/L)	18.22	0.02	0.17	ND	1.98	0.21	4.57	0.55
	Glycerol equivalent[b] (g/L)	–	–	0.13	–	3.09	0.26	9.14	0.85
	Metabolite distribution[c] (%)	–	–	0.99	–	22.94	1.95	67.81	6.31
	Glycerol efficiency[d] (%)	73.92	–	–	–	–	–	–	–

ND not detected

[a] Total concentration of glycerol consumption, biomass concentration (g-DCW/L), and major metabolite concentrations for each specific stage of the fed-batch culture

[b] Calculated based on theoretical yield of each metabolite to glycerol (Fig. 1b)

[c] Represents the fraction of dissimilated glycerol

[d] Ratio of the sum of the glycerol equivalents associated with all metabolites to overall glycerol consumption

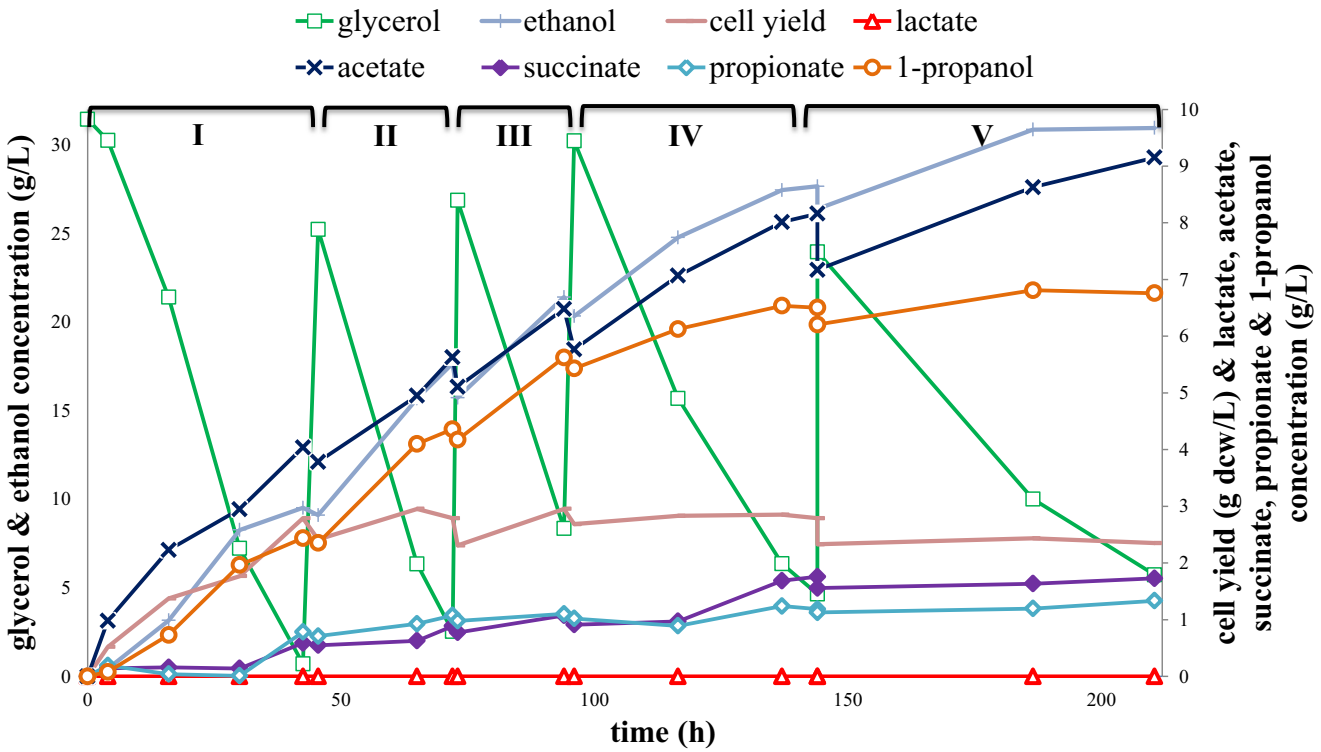

Fig. 7 Time profiles of the concentrations glycerol, biomass, and major metabolites during fed-batch cultivation of CPC-PrOH3 with glycerol as the major carbon source. Approximately 25 g of pure glycerol was fed into the bioreactor in the beginning of each stage and samples were taken before and after the glycerol feeding

after Stage I (Figs. 6 and 7). The mechanism associated with this rate increase is unknown, but may entail the induction of genes responsible for glycerol dissimilation (e.g., *gldA*, encoding glycerol dehydrogenase and *dhaKLM*, encoding a PEP-dependent dihydroxyacetone kinase) (Murarka et al. 2008) and/or the formation of certain intermediate metabolites which may act as external electron donors. Since synthesis of ethanol and succinate (and 1-propanol in the present study) are the only pathways readily available for redox-balancing during glycerol fermentation (Dharmadi et al. 2006), the elevated rate of glycerol consumption was concomitant with the increase in conversion yields of ethanol and succinate during Stages II and III (Table 2). However, given that the ethanologenic pathway leads to higher ATP output (Fig. 1a) (da Silva et al. 2009), more than 60 % (and up to 75 %) of dissimilated glycerol was diverted to ethanol production, whereas less than 15 % was diverted to succinate and 1-propanol production (Table 2, and Fig. 8). Such high-level production of ethanol sustained during almost the entire fed-batch cultivation and, therefore, limited 1-propanol yield. Taken together, these results suggest that further enhancement of 1-propanol production with glycerol as the major carbon source will require sequestering of carbon flux from the ethanologenic pathway. For example, placing an entropic driving force at the PEP node through the expression of a heterologous PEP carboxykinase (PckA) (Song and Lee 2006) or converting pyruvate back to PEP through the expression of an endogenous phosphoenolpyruvate synthase (Pps) (Chao et al. 1993) may be feasible approaches to shift carbon flux from ethanologenesis toward 1-propanol production. On the other hand, the recession of 1-propanol production in later stages of fed-batch cultures correlated with heightened levels of acetate and ethanol production (Figs. 6, 7, and 8), suggesting that the toxicity of these metabolites may mediate physiological stresses on cells and eventually hinder 1-propanol production.

While ethanol can be the exclusive product of glycerol fermentation (accounting for ~98 % glycerol equivalents) by wild-type *E. coli* strains (Murarka et al. 2008), our fed-batch cultivation with glycerol as the major carbon source produced acetate in relatively large quantities (Figs. 6 and 7). Figure 8 shows that, across all time periods of the fed-batch cultivation, the average carbon flux for acetate production was greater than or approximately equal to that for 1-propanol production. A simple explanation to this observation can be derived from the redox balance associated with glycerol dissimilation. No net NADH is produced when glycerol is converted to ethanol, whereas the overall conversion of glycerol to acetate and 1-propanol will result in 2 NADH accumulation and 2 NADH depletion, respectively. Shifting carbon flux away from

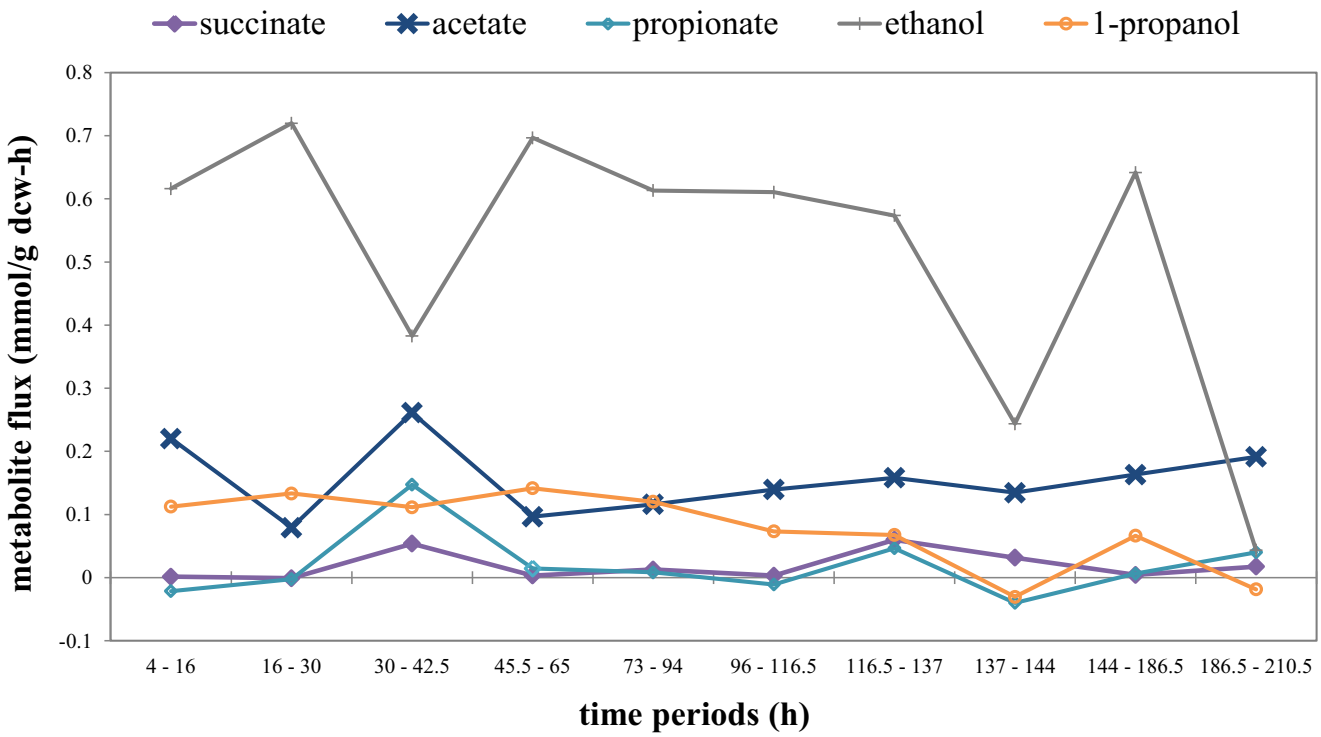

Fig. 8 Average metabolite excretion fluxes during each stage of CPC-PrOH3 cultivation (Fig. 7). The fluxes were estimated by normalizing the glycerol uptake rate to 1 mmol/g DCW-h. While most carbon flux was channeled into the ethanol fraction, 1-propanol production was stably maintained throughout the entire cultivation

ethanol pathway and toward 1-propanol production would cause NADH imbalance, which can be partially compensated by concomitant production of acetate. Note that extra ATP will be released upon acetate production to support potential ATP requirement for cell growth and maintenance. This is evident in the late stages of batch cultivations (Fig. 5), as cultures tend to suffer from overflow metabolism of acetate in order to fulfill cell maintenance requirements.

Multicopy plasmids tend to place metabolic burden and physiological impact on host cells, deteriorating cell growth and product formation. Unlike overexpression of recombinant proteins, gene dosage is seldom a limiting factor for metabolic engineering approaches (Jones et al. 2000), for which plasmid-free strains are particularly attractive. The Sbm operon in *E. coli* is naturally silent, conceivably due to a weak or inactive promoter-operator system (Kannan 2008; Leadlay 1981), thus providing us with a unique opportunity for minor genomic engineering without grafting several heterologous genes or a large operon into the host genome. In the present study, we derived a plasmid-free propanogenic strain CPC-PrOH3 for which expression of the Sbm operon was activated by replacing the 204-bp upstream region of the native Sbm operon with the strong *trc*-promoter. Compared to CPC-PrOH2, CPC-PrOH3 has the following technical advantages, leading to high-level coproduction of 1-propanol and ethanol. First, CPC-PrOH3 had higher rates for cell growth and glycerol dissimilation (Fig. 7), potentially due to alleviated metabolic burden and more active expression of the Sbm operon (even based on a single chromosomal copy). Second, upon glycerol fermentation, CPC-PrOH3 had a higher level of solventogenesis (accounting for up to 85 % of dissimilated glycerol), a higher 1-propanol conversion yield (accounting for up to 14 % of dissimilated glycerol), and a prolonged 1-propanol producing capacity during the fed-batch culture (particularly during the first three stages) (Table 2). The results suggest that a single chromosomal copy of the active Sbm operon was sufficient to drive extended dissimilation of succinate for effective 1-propanol production. Also, alleviating the metabolic burden associated with the presence of multicopy plasmids can lead to healthy cell physiology and, consequently, improved production of the target metabolite. While the dominance of ethanologenesis upon glycerol fermentation remains the key issue to be tackled, 1-propanol production for CPC-PrOH3 can be potentially limited by the accumulation of acetate and succinate. These limitations along with the decreasing glycerol utilization efficiency for metabolite production (Table 2) suggest metabolic burden might still exist in CPC-PrOH3, leading to inactivation of the Sbm operon, particularly toward the late stage of the fed-batch culture. Interestingly, although CPC-PrOH3 had a fully activated Sbm operon (including *ygfH*), propionate production appeared to be minimally affected when compared to the fed-batch culture of CPC-PrOH2 (in which the episomal construct only includes the *sbm*, *ygfD*, and *ygfG* genes). These results

suggest that either propionyl-CoA may have a higher substrate affinity toward bifunctional alcohol/aldehyde dehydrogenases than YgfH or other pathways may exist in *E. coli* to facilitate the conversion of propionate to propionyl-CoA. One possibility is the canonical methylcitrate pathway, which is involved in the oxidation of propionate to pyruvate or succinate with propionyl-CoA as an intermediate (Brock et al. 2002).

Acknowledgments The authors' research is supported by the Natural Sciences and Engineering Research Council (NSERC) and the Canada Research Chair (CRC) program of Canada. The authors would like to thank Zhimeng Yu for providing technical assistance in flux balance analysis.

References

Amann E, Ochs B, Abel K-J (1988) Tightly regulated *tac* promoter vectors useful for the expression of unfused and fused proteins in *Escherichia coli*. Gene 69:301–315

Atsumi S, Cann AF, Connor MR, Shen CR, Smith KM, Brynildsen MP, Chou KJY, Hanai T, Liao JC (2008a) Metabolic engineering of *Escherichia coli* for 1-butanol production. Metab Eng 10:305–311

Atsumi S, Hanai T, Liao JC (2008b) Non-fermentative pathways for synthesis of branched-chain higher alcohols as biofuels. Nature 451:86–89

Baba T, Ara T, Hasegawa M, Takai Y, Okumura Y, Baba M, Datsenko KA, Tomita M, Wanner BL, Mori H (2006) Construction of *Escherichia coli* K-12 in-frame, single-gene knockout mutants: the Keio collection. Mol Syst Biol 2:1–11

Barnard RT (2005) Chimerization of multiple antibody classes using splice overlap extension PCR. BioTech 38:181–182

Brock M, Maerker C, Schütz A, Völker U, Buckel W (2002) Oxidation of propionate to pyruvate in *Escherichia coli*. Eur J Biochem 269: 6184–6194

Casadaban MJ (1976) Transposition and fusion of the lac genes to selected promoters in *Escherichia coli* using bacteriophage lambda and Mu. J Mol Biol 104:541–555

Chao Y, Patnaik R, Roof W, Young R, Liao J (1993) Control of gluconeogenic growth by pps and pck in *Escherichia coli*. J Bacteriol 175:6939–6944

Cherepanov PP, Wackernagel W (1995) Gene disruption in *Escherichia coli*: Tc^R and Km^R cassettes with the option of Flp-catalyzed excision of the antibiotic-resistance determinant. Gene 158:9–14

Cintolesi A, Clomburg JM, Rigou V, Zygourakis K, Gonzalez R (2012) Quantitative analysis of the fermentative metabolism of glycerol in *Escherichia coli*. Biotechnol Bioeng 109:187–198

Clomburg JM, Gonzalez R (2011) Metabolic engineering of *Escherichia coli* for the production of 1,2-propanediol from glycerol. Biotechnol Bioeng 108:867–879

da Silva GP, Mack M, Contiero J (2009) Glycerol: a promising and abundant carbon source for industrial microbiology. Biotechnol Adv 27:30–39

Datsenko KA, Wanner BL (2000) One-step inactivation of chromosomal genes in *Escherichia coli* K-12 using PCR products. Proc Natl Acad Sci U S A 97:6640–6645. doi:10.1073/pnas.120163297

Deng Y, Fong SS (2011) Metabolic engineering of *Thermobifida fusca* for direct aerobic bioconversion of untreated lignocellulosic biomass to 1-propanol. Metab Eng 13:570–577

Dharmadi Y, Murarka A, Gonzalez R (2006) Anaerobic fermentation of glycerol by *Escherichia coli*: a new platform for metabolic engineering. Biotechnol Bioeng 94:821–829

Fernando S, Adhikari S, Kota K, Bandi R (2007) Glycerol based automotive fuels from future biorefineries. Fuel 86:2806–2809

Fiege H, Voges H, Hamamoto T (2002) Ullmann's encyclopedia of industrial chemistry. Federal Republic of Germany, AG Bayer 19: 324

Froese D, Dobson C, White A, Wu X, Padovani D, Banerjee R, Haller T, Gerlt J, Surette M, Gravel R (2009) Sleeping beauty mutase (*sbm*) is expressed and interacts with *ygfd* in *Escherichia coli*. Microbiol Res 164:1–8

Glick BR (1995) Metabolic load and heterologous gene expression. Biotechnol Adv 13:247–261

Haller T, Buckel T, Rétey J, Gerlt JA (2000) Discovering new enzymes and metabolic pathways: conversion of succinate to propionate by *Escherichia coli*. Biochemistry 39:4622–4629

Hanahan D (1983) Studies on transformation of *Escherichia coli* with plasmids. J Mol Biol 166:557–580

Jain R, Yan Y (2011) Dehydratase mediated 1-propanol production in metabolically engineered *Escherichia coli*. Microb Cell Factories 10:1–10

Jantama K, Zhang X, Moore J, Shanmugam K, Svoronos S, Ingram L (2008) Eliminating side products and increasing succinate yields in engineered strains of *Escherichia coli* C. Biotechnol Bioeng 101: 881–893

Jarboe LR, Zhang X, Wang X, Moore JC, Shanmugam K, Ingram LO (2010) Metabolic engineering for production of biorenewable fuels and chemicals: contributions of synthetic biology. J Biomed Biotechnol 2010:1–18

Jobling MG, Holmes RK (1990) Construction of vectors with the pl5A replicon, kanamycin resistance, inducible lacZα and pUC18 or pUC19 multiple cloning sites. Nucleic Acids Res 18:5315–5316

Jones KL, Kim S-W, Keasling J (2000) Low-copy plasmids can perform as well as or better than high-copy plasmids for metabolic engineering of bacteria. Metab Eng 2:328–338

Jun Choi Y, Hwan Park J, Yong Kim T, Yup Lee S (2012) Metabolic engineering of *Escherichia coli* for the production of 1-propanol. Metab Eng 5:477–486

Kannan SM (2008) Studies on methylmalonyl-CoA mutase from *Escherichia coli*. University of Westminster

Korz D, Rinas U, Hellmuth K, Sanders E, Deckwer W-D (1995) Simple fed-batch technique for high cell density cultivation of *Escherichia coli*. J Biotechnol 39:59–65

Leadlay PF (1981) Purification and characterization of methylmalonyl-CoA epimerase from *Propionibacterium shermanii*. Biochem J 197: 413

Miller JH (1992) A short course in bacterial genetics: a laboratory manual and handbook for *Escherichia coli* and related bacteria, vol 1. Cold Spring Harbor Laboratory Press

Murarka A, Dharmadi Y, Yazdani SS, Gonzalez R (2008) Fermentative utilization of glycerol by *Escherichia coli* and its implications for the production of fuels and chemicals. Appl Environ Microbiol 74: 1124–1135

Neidhardt FC, Bloch PL, Smith DF (1974) Culture medium for enterobacteria. J Bacteriol 119:736–747

Ow DS-W, Nissom PM, Philp R, Oh SK-W, Yap MG-S (2006) Global transcriptional analysis of metabolic burden due to plasmid maintenance in *Escherichia coli* DH5α during batch fermentation. Enzym Microb Technol 39:391–398

Rase HF (2000) Handbook of commercial catalysts: heterogeneous catalysts. CRC, Boca Raton

Shen CR, Liao JC (2008) Metabolic engineering of *Escherichia coli* for 1-butanol and 1-propanol production via the keto-acid pathways. Metab Eng 10:312–320

Shen C, Liao J (2013) Synergy as design principle for metabolic engineering of 1-propanol production in *Escherichia coli*. Metab Eng 17:12–22

Song H, Lee SY (2006) Production of succinic acid by bacterial fermentation. Enzym Microb Technol 39:352–361

Srirangan K, Akawi L, Moo-Young M, Chou CP (2012) Towards sustainable production of clean energy carriers from biomass resources. Appl Energy 100:172–186

Srirangan K, Akawi L, Liu X, Westbrook A, Blondeel EJ, Aucoin MG, Moo-Young M, Chou CP (2013) Manipulating the sleeping beauty mutase operon for the production of 1-propanol in engineered *Escherichia coli*. Biotechnol Biofuels 6:139

Sukhija K, Pyne M, Ali S, Orr V, Abedi D, Moo-Young M, Chou CP (2012) Developing an extended genomic engineering approach based on recombineering to knock-in heterologous genes to *Escherichia coli* genome. Mol Biotechnol 51:109–118

van de Walle M, Shiloach J (1998) Proposed mechanism of acetate accumulation in two recombinant *Escherichia coli* strains during high density fermentation. Biotechnol Bioeng 57:71–78